Design of poured earth construction materials from the elementary characteristics of tropical soils

Lily Walter, Yannick Estevez, Gildas Medjigbodo, Jean-Emmanuel Aubert, Laurent Linguet, Ouahcène Nait-Rabah

Case Studies in Construction Materials 20 (2024) e02709

Contents lists available at ScienceDirect

Case Studies in Construction Materials

journal homepage: www.elsevier.com/locate/cscm

Design of poured earth construction materials from the elementary characteristics of tropical soils

Lily Walter [a,*], Yannick Estevez [b], Gildas Medjigbodo [a], Jean-Emmanuel Aubert [c], Laurent Linguet [d], Ouahcène Nait-Rabah [a]

[a] UMR EcoFog, Université de Guyane, Kourou, French Guiana
[b] CNRS, UMR EcoFoG, Université de Guyane, Cayenne, French Guiana
[c] LMDC, Université de Toulouse, INSA/UPS Génie Civil, 135 Avenue de Rangueil, 31077 Toulouse cedex 04, France
[d] UMR Espace-DEV, IRD, Université de la Guyane, Cayenne, French Guiana

ARTICLE INFO

Keywords:
Poured earth
Dispersant
Tropical soils

ABSTRACT

Sustainable construction materials and local solutions are crucial for meeting urbanisation demands in tropical regions like French Guiana. Poured earthen construction, primarily composed of local soil, offers a cost-effective and environmentally friendly alternative. To ensure good consistency for pouring, the use of dispersants to deflocculate clay particles is an effective strategy that reduces water demand while enhancing the material's physical and mechanical properties. However, the variability of soil impacts the effectiveness of dispersants and the earth's material properties. It is currently unknown how the specific properties of tropical soils can influence the mix design of poured earth and how it impacts their resulting physical and mechanical characteristics. This work examines the soil properties that could help select suitable soil for poured earth construction. Four tropical soils of French Guiana were characterised in detail and used to prepare mortars with varying amounts of water and dispersant (sodium hexametaphosphate). The consistency and compressive strength of the mortars correlated with the mineralogical and geotechnical characteristics of the soils. In particular, soils with high levels of metal oxides produced mortars with the highest compressive strength. Using a dispersant consistently increased the compressive strength and dry density of the mortars and enabled a reduction in water content. Importantly, the analysis revealed that two easily measurable soil properties, the passing at 63 μm and the pH measured in potassium chloride (pH KCl), could predict the mechanical properties of the mortars and the amount of dispersant needed. Specifically, the pH KCl correlated with the proportion of iron and aluminium oxide and showed a positive linear correlation with the compressive strength. Overall, this study identifies easily measurable soil properties, in particular the pH KCl, for selecting and designing high-performance earth materials with tropical soils. It offers promising prospects for industrialising poured earth construction.

1. Introduction

Rapid urbanisation in tropical regions in South America, such as French Guiana or elsewhere in Africa and Asia, requires new sustainable construction techniques to reduce resource consumption and greenhouse gas emissions [1]. Earth construction represents

* Corresponding author.
E-mail address: lily.walter@etu.univ-guyane.fr (L. Walter).

https://doi.org/10.1016/j.cscm.2023.e02709
Received 16 October 2023; Received in revised form 17 November 2023; Accepted 22 November 2023
Available online 24 November 2023

an attractive solution due to its local availability, abundance, minimal environmental impact, and high recyclability [2,3]. Specifically, the hygrothermal properties of earth materials can improve thermal comfort and reduce the energy required for air conditioning in tropical regions [4]. Despite the advantages of earthen materials, traditional earth construction techniques are time-consuming, labour-intensive, and possess reduced mechanical properties and durability. Additionally, they are highly dependent on soil variability, limiting their widespread adoption in the construction industry [5]. Thus, developing modern earth construction techniques that adapt to soil variability is critically needed.

Earth materials are primarily composed of soil. Soils are made of gravel, sand, and silt, forming the granular skeleton, and clay, the finest fraction, that acts as the cohesive binding phase. Soil mineralogical and geotechnical properties are related to their geological history and can vary significantly, even within a relatively small area [6–9]. As a result, earth materials exhibit inconsistent performance. To better understand and control this variability, recent research has focused on identifying essential soil properties critical for selecting and designing high-strength earthen materials [10–16].

Shrinkage and rheological characteristics of earth materials are strongly correlated with soil properties such as the Atterberg limit, particle size, and solid volume fraction [10–12,17]. The strength of earthen materials is attributed to capillary forces and ionic interactions between clay particles and are influenced by the soil's specific surface area and cation exchange capacity [10–12,18]. However, most studies have been performed using moderately weathered soils in temperate climates, and it is unknown whether these findings also apply to highly weathered tropical soils.

In temperate climates, the clay fraction is usually composed of phyllosilicates and consists of sheets of aluminosilicate carrying a negative charge on their large basal face. As a result, these soils have a net negative charge and can retain cations, which can be assessed by the cation exchange capacity or the methylene blue test. By contrast, in highly weathered soils in tropical and humid climates, the clay fraction typically contains high levels of metal oxides in addition to phyllosilicates, mainly aluminium and iron. These metal oxides can carry variable charges, either positive or negative, depending on the pH and ionic strength of the soil [19]. In tropical soils, which typically have acidic pH (pH < 7), metal oxides carry positive charges and absorb onto the negative basal face of phyllosilicate, causing clay particles to form durable aggregates that reinforce soil structure [19,20]. When metal oxides cover all the negative charges of phyllosilicate, they can generate a net positive charge. This charge can be measured using the anion exchange capacity test. However, measuring anion exchange capacity is a complex procedure not commonly conducted in soil laboratories [21]. Alternatively, a simple method comparing the pH in water and in potassium chloride (KCl) provides information on soil charge. In most soils, the pH is lower in KCl solutions than in water, except for certain acidic, weathered tropical soils where the opposite occurs [22]. A ΔpH (pH KCl - pH water) < 0 indicates a net negative charge (cation exchange capacity), while a ΔpH > 0 indicates a net positive charge (anion exchange capacity). Measuring soil pH in water and KCl holds promise for rapidly assessing soil charge in tropical soils [22,23], as shown later in this manuscript.

Poured earth construction is easy to shape and could become a popular alternative to traditional cement concrete [24–28]. Similar to cement concrete, poured earth construction requires adequate fluidity during the initial stage for casting within formworks, followed by rapid solidification. To achieve fluid consistency, earth materials, when used without additives, require a substantial water content, resulting in low strength and high shrinkage after drying [2,29]. Consequently, dispersants are commonly employed to deflocculate the clay fraction, enabling fluid consistency, reducing water content, enhancing density and strength, and decreasing shrinkage [24,30–33]. Dispersants are chemical species that adsorb on the surface of clay particles and generate repulsive forces between them, leading to deflocculation. Sodium hexametaphosphate (NaHMP) is one of the most commonly used dispersants and has shown high efficiency in deflocculating various soil types [25,26,29,31,34,35], including tropical soil [9]. However, the efficiency of NaHMP is highly dependent on the amount used, the type and the quantity of clay [13,32,36,37]. Studies showed that increasing NaHMP content improved consistency until reaching a maximal deflocculated state, after which further increases had a limited effect on consistency but notably decreased compressive strength [38]. Therefore, to achieve maximum strength and water reduction in poured earth, it is necessary to precisely adjust the amount of NaHMP based on the soil type.

The present study aims to identify tropical soil properties that influence the design of poured earth mixes and their resulting physical and mechanical characteristics. The geotechnical and mineralogical properties of four soils were characterized and used to prepare mortar with varying concentrations of water and NaHMP. First, the goal was to establish a relationship between soil properties and the properties of plastic earth mortars made at different levels of water content without dispersant. Second, the effect of increasing NaHMP content on mortar consistency was evaluated and related to soil properties. Third, poured earth mortars with an adjusted NaHMP content and a reduced water content was prepared and compared to the plastic earth mortars.

2. Materials and methods

2.1. Materials

2.1.1. Soils and dispersant

Four soils were collected from three different lateritic quarries located along the coast of French Guiana. The soils, named K, S, M1, and M2, were respectively collected near Kourou, Sinamary, and Mana. According to the geological maps of French Guiana [39], soils K and S were classified as ancient metamorphic rocks and described as amphibolite and Orapu Schist, respectively. M1 and M2 were collected from the same quarry used by a local company that provides cement-stabilised compressed earth bricks (SCEBs). These soils were classified as marine and fluviomarine depositions [39]. These two soils were collected approximately fifty meters apart at similar depths to assess soil variability within the same quarry. Each soil was air-dried and sieved to a 2 mm size. The remaining clay agglomerates were mechanically crushed with a disaggregating mixer employed in Proctor test NF P94–093 and sieved again. The

passing 0–2 mm soil was used for all the characterisation and mortar preparation.

Sodium hexametaphosphate $(NaPO_3)_6$, 98.0% pure in powder sourced from ThermoFisher, was used as the clay dispersant, and referred to as NaHMP.

2.1.2. Mix design

Mortars were constituted of different proportions of soil, water and NaHMP. A three-step methodology was proposed to formulate high-strength poured earth mortars.

1. Establishing the Optimum Water Content **OWC:** Different plastic earth mortars prepared without dispersant at increasing water content were characterised. The OWC corresponded to the water content producing the maximum compressive strength of the hardened mortar.
2. Establishing the optimum **$NaHMP_{opt}$** content: The consistency of fresh mortars made at their OWC was tested with increasing concentrations of NaHMP. The $NaHMP_{opt}$ corresponded to the minimal concentration of NaHMP sufficient to obtain a yield stress of 4 Pa. This yield stress value was based on a previous study that showed that increasing NaHMP concentration decreased the yield stress until it reached a critical yield stress of 4 Pa, corresponding to the maximum deflocculated state [38]. Beyond this point, higher NaHMP concentration had a limited impact on yield stress but substantially decreased compressive strength [38].
3. Establishing a suitable pouring water content **PWC** for a mix of soil and $NaHMP_{opt}$: The PWC of a mortar composed of soil and $NaHMP_{opt}$ was defined by adjusting the consistency to enable the pouring of the mortar. This consistency was fixed at a yield stress of 1000 Pa, which enables easy pouring and could be used for vibrated poured walls [40–42].

2.2. Methods

2.2.1. Soil characterisation

All chemical and mineralogical characterisations were performed on crushed samples smaller than 80 μm. The major oxide composition was evaluated using Inductively Coupled Plasma-Optical Emission Spectrometry (ICP-OES). The loss on ignition (L.O.I.) was determined at 1000 °C. Soil pH in distilled water and in 1 M KCl (soil solution ratio 1: 2.5) was measured using a standard pH electrode after 1 h of stirring and 24 h of resting [43].

Crystalline compounds were identified using an X-ray diffractometer (XRD) equipped with a Soller monochromator and a copper anticathode ($\lambda = 1.54$ Å), specifically a Bruker D8 Advance X-ray diffractometer. Thermo-Gravimetric Analysis (TGA) was conducted on crushed samples heated to 1000 °C at a constant rate of 10 °C/min using a Netzsch SATA 449 F3 Jupiter apparatus.

The particle size was determined using standard methods: XP P94–056 for the coarser fraction (80–2000 μm) using dry sieving after washing and XP P94–057 for the finer fraction (<80 μm) using the hydrometer testing. The Atterberg limit was determined on the passing at 400 μm according to ISO 17892–12, with the liquid limit determined using the cone penetrometer test. The plasticity index was calculated by subtracting the plastic limit from the liquid limit. The methylene blue adsorption test was conducted following the NF P 94–068. The specific surface areas were determined by applying the Brunauer-Emmett-Teller (BET) theory under a nitrogen atmosphere. The Flowsorb 2300 equipment (Micromeritics) was used to obtain single-point BET surface area measurements.

2.2.2. Mortar preparation and characterisation

All mortars were prepared using the same procedure. The soil was mixed with distilled water for 3 min at a low speed of 62.5 rpm, followed by 3 min at a high speed of 125 rpm. When NaHMP was used, it was dissolved in distilled water. Subsequently, the consistency of the fresh mortar was assessed by evaluating the mortar yield stress as described in the following section. Afterwards, the water content was controlled by standard ISO 17892–1. The mixture was poured into lubricated $4\times4\times16$ cm^3 moulds and stored under laboratory uncontrolled conditions. Moulds were removed at 72 h, and mortar prisms dried under the same condition until reaching a stable mass to characterise the hardened mortar.

The fresh mortar consistency was evaluated by measuring the yield stress by conducting two tests: the cone penetrometer test for the plastic consistency and the slump and spread test for the fluid consistency. The cone penetrometer test, a widely used test to determine the liquid limits of soils, has proven effective in determining the yield stress of fresh mortar with a plastic consistency [44,45]. The procedure involved filling a 45 mm high mould with the fresh mortar and dropping a cone (80 g/30°/35 mm height) for 5 s. The penetration depth is then recorded and used to calculate the yield stress in the 100–0.75 kPa range, as described in [46]. For accuracy, the fresh mortar paste must be homogeneous, and the largest grain size should not exceed 10% of the cone's height [45]. The equation used to calculate the yield stress was described previously [45].

The slump and spread test using the Abrams cone is a standard method to evaluate the consistency of fluid mortar. It has demonstrated its suitability to evaluate the yield stress of fluid mortar consistency [47]. This study used a reduced-size Abrams cone with dimensions two times smaller in a homothetic ratio than the standard Abrams cone (height 15 cm, $Ø_1$ =5 cm, $Ø_2$ =10 cm). The procedure has been adapted from previous studies [48,49]. It involves moistening the cone, placing it on a flat, wet metal surface, filling the cone in two layers, each stitched 15 times with a 1.6 cm-diameter metal needle, removing excess mortar and finally, lifting the cone vertically in less than 2 s and record the final slump and spreading diameter when the flow stops. The slump and spread measures were used to calculate the mortar yield stress in the range 1500 – 2 Pa as described in [47]. Both tests were performed three times, and the yield stress's mean value and standard deviation were calculated. While not exact methods, these methods provide a reliable measure of the yield stress that can be used to compare samples between experiments.

Several properties of the hardened mortars were measured, including volumetric shrinkage, dry density, and compressive strength.

The volume and dry density were measured with a calliper (± 0.05 mm) and balance (± 0.05 g). Dry density was calculated for the hardened specimen's moisture content. Volumetric shrinkage was expressed as the mean percentage volumetric variation between the fresh and hardened state of the three 4 × 4 × 16 cm^3 specimens. The compressive strength was tested at a constant speed of 50 N/s and using a 10 kN or 300 kN sensor, depending on the strength.

3. Results and discussion

3.1. Soil characterisation

3.1.1. Chemical characterisation

The chemical compositions obtained through ICP-AES and loss on ignition at 1000 °C of the four soils studied are presented in Table 1. As expected for weathered tropical soil, the four soils were mainly composed of silica, and aluminium and iron oxides [6]. Soil M1 and M2 were collected from the same quarry and had a very similar composition, with high quantities of silica (> 64%) and low quantities of aluminium (< 16%) and iron oxides (< 10%). By contrast, soils K and S had a lower silica content (< 37%) but higher aluminium (> 26%) and iron oxides (>19%). A low amount of titanium was also found in all the soils, ranging from 1% to 5%. All the other studied oxides were either absent or present in very low quantities (<0.5%), with the exception of Magnesium in soil S (0.8%).

The soil pH was measured either in distilled water or in a solution of 1 M KCl. ΔpH (pH water - pH KCl) was calculated and presented in Table 1. As expected for tropical soils with heavy rainfall and heavy leaching, the four soils had acidic pH comprised between 4 and 5.5 either in water or KCl [6]. Measuring the ΔpH provide an easy measurement of the net charge of the soil. The added cations (K^+) and anions (Cl-) interact with the H^+, Al^{3+} and OH^- terminations of the soil solid surfaces. In negatively charged soils, K^+ ions replace H^+ and Al^{3+} ions on the basal face of the phyllosilicate, lowering the pH and leading to a ΔpH < 0. By contrast, in positively charged soils, Cl^- ions replace the OH^- present on metal oxides, which increases the pH and leads to a ΔpH > 0 [22]. Soil K and S showed a positive ΔpH, revealing a net positive charge, which is consistent with the high metal oxide content of these two soils. Conversely, the metal poor M1 and M2 soils showed a negative ΔpH, indicative of a net negative charge.

Importantly, the total metal oxide content exhibited a strong positive linear correlation with the pH KCl (R^2 =0.99) but not with the pH water (R^2 =0.48) (Fig. 1). A correlation between pH and metal oxide has been observed in several studies on tropical soil [23, 50–52]. It is attributed to the inhibition of acidification generated by amorphous iron, aluminium oxides, and Fe/Al coating on kaolinite through electrical double-layer interactions [50,53,54]. Importantly, this correlation suggests that a quick and cost-effective evaluation of the pH KCl could accurately indicate the proportion of metal oxide in tropical soils.

3.1.2. Mineralogical characterisation

The X-ray diffractograms of the four soils are presented in Fig. 2. All the diagrams revealed the strong presence of kaolinite *($Al_2(Si_2O_5)(OH)_4$)* and quartz *(SiO_2)*. Several types of iron and aluminium oxides were observed. Goethite *(FeO(OH))* was identified in soils K, M1, and M2. Al-goethite *($Fe_{0.83}Al_{0.17}O(OH)$)* was identified in soil S. Hematite *(Fe_2O_3)* was identified in soils M1, M2, and S. Gibbsite *($Al(OH)_3$)* was identified in soils K, M1, and S, diaspore *(AlO(OH))* in soil M2 and S. Furthermore, a spinel F *($Mg(Al,Fe)O_3$)* was identified in soil S and could explain the detectable presence of magnesium measured by ICP-OES (Table 1). Muscovite was also present in soil S, as confirmed by visually observing shiny grains.

Mineralogical characterisation was completed by thermo-gravimetric analysis (Fig. 3).

In the four soil samples, three ranges of mass loss were identified. The first mass loss occurred between 80 and 160 °C and corresponded to the evaporation of water. This hygroscopic water evaporation was greater for soils K and S and was attributed to the high proportion of iron and aluminium oxides in these soils, which exhibit a strong affinity for water [55]. The second range of mass loss occurred around 300 °C and corresponded to the dihydroxylation of goethite, gibbsite, and diaspore species. This mass loss showed higher intensity in soils K and S than in soils M1 and M2, which aligned with the results obtained from the ICP-OES analysis. The third mass loss occurred around 500 °C and corresponded to the removal of constitutive water from kaolinite as observed in the X-ray diffractogram. Soil K showed the highest mass loss, followed by soil M2, M1, and S.

A potential mineralogical composition was deducted by combining the chemical composition measured by ICP-OES and L.O.I with the mineral composition evaluated through X-ray diffraction and thermo-gravimetric analyses (Table 2).

The X-ray diffraction analysis provided qualitative information regarding crystallised minerals in the samples. The chemical composition and thermo-gravimetric analysis were used for quantitative analysis by assigning certain elements to specific minerals. Of note, it required strong assumptions regarding the chemical formulas of minerals that can be highly variable. An iterative process was employed to fulfil the majority of the experimental requirements. Most likely compositions resulting from this process are presented in Table 2. Soil K was mainly composed of kaolinite and goethite. The two soils collected from the Mana quarry (M1, M2) were highly

Table 1
Soil chemical properties.

	SiO_2	Al_2O_3	Fe_2O_3	MnO	MgO	CaO	Na_2O	K_2O	TiO_2	P_2O_5	L.O. I	Total	pH water	pH KCl	ΔpH
K	28.7	27.0	24.1	0.1	< 0.1	< 0.1	< 0.1	< 0.1	4.5	0.1	14.4	98.9	4.96	5.12	0.16
M1	75.4	12.1	6.4	< 0.1	< 0.1	< 0.1	< 0.1	0.1	1.4	< 0.1	5.3	100.7	4.96	4.24	- 0.72
M2	64.9	15.7	10.0	< 0.1	< 0.1	< 0.1	< 0.1	0.2	1.6	< 0.1	6.8	99.2	4.58	4.29	- 0.29
S	36.1	29.2	19.2	< 0.1	0.8	< 0.1	0.3	0.3	2.0	< 0.1	11.2	99.2	5.32	5.43	0.11

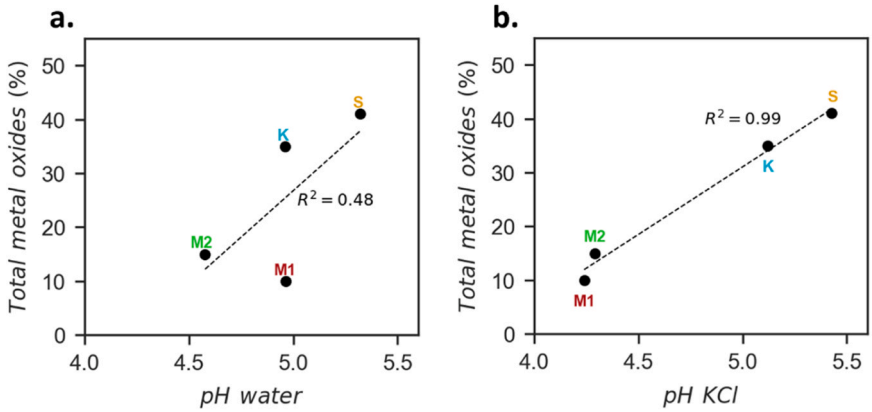

Fig. 1. Correlation between the total metal oxide content and the pH water (a) and the pH KCl (b).

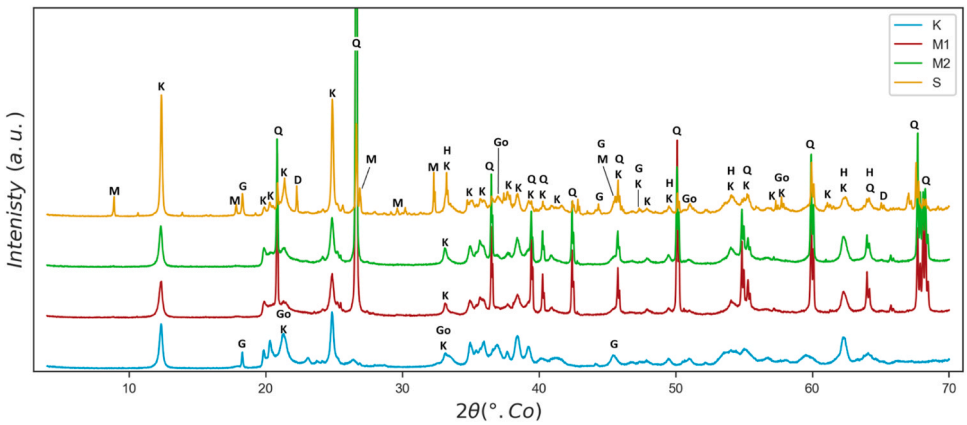

Fig. 2. X-ray diffraction patterns of the four soils. D: Diaspore, G: Gibbsite, Go: Goethite, H: Hematite, M: Muscovite, Q: Quartz, K: Kaolinite.

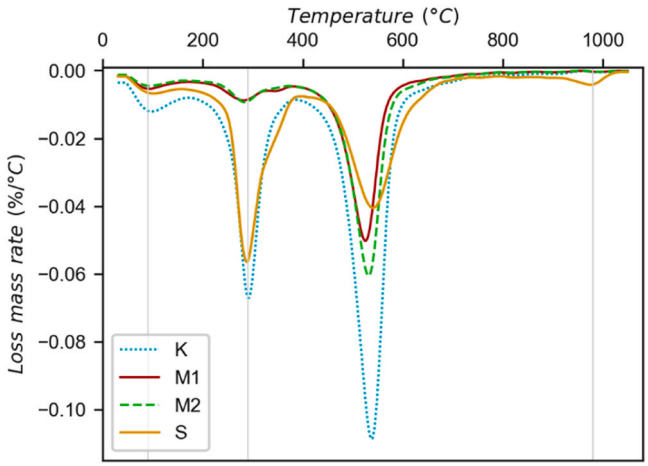

Fig. 3. Derivative thermo-gravimetric curves.

Table 2
Soil potential mineralogical composition.

	K	M1	M2	S
Quartz - SiO_2	1	62	49	19
Phyllosilicates:				
Kaolinite (%) - $Al_2(Si_2O_5)(OH)_4$	61	28	35	34
Muscovite (%) - $KAl_2(AlSi_3O_{10})(OH,F)_2$	0	0	0	3
Iron oxides:				
Hematite (%) - Fe_2O_3	0	2	4	14–18
Goethite (%) - FeO(OH)	25	5	7	0
Goethite Al (%) - $Fe_{0.83}Al_{0.17}O(OH)$	0	0	0	0–5
Aluminium oxides:				
Gibbsite (%) - $Al(OH)_3$	5	1	0	7–9
Diaspore (%) - AlO(OH)	0	0	2	9–10
Spinel F (%) - $Mg(Al, Fe)O_3$	0	0	0	3
Other oxides:	5	2	2	2
Total phyllosilicates	61	28	35	37
Total metal oxides	35	10	15	35–47

similar and were composed mainly of quartz and kaolinite. On the other hand, soil S demonstrated a more diverse composition, with approximately one-third of kaolinite and similar quantities of quartz, iron, and aluminium oxide, at around 20% each.

3.1.3. Geotechnical characterisation

Table 3 presents the geotechnical characterisation of the four soils, including particle size, median grain diameter values (D50), texture, Atterberg limit, methylene blue test, and the specific surface area. Data show mean and standard deviation from three independent measurements.

(in red: Soil properties exceeding the recommended threshold range).

The particle size distribution of the four soils is presented in Fig. 4.

The clay content ranged from 19.6% to 50.5%, silt from 9.4% to 42.5% and sand from 7.3% to 58.9%. Of important note, the aggregation of iron and aluminium oxides with kaolinite can result in an underestimation of the clay content in favour of increased silt and sand contents in iron-rich tropical soils [58,59]. Thus, the high silt fraction of approximately 40% observed in the metal oxide-rich soil K and S may be an overestimation at the expense of the clay fraction.

The Atterberg limits are often used to assess soil suitability for earthen construction. The plasticity limit represents the water content needed to transition from a solid to a plastic consistency, and the liquid limits the water content needed to transition from a plastic to a liquid state. The liquid limit of the four soils ranged from 44.1% to 72.9%, the plasticity limit from 22.3% to 44.9% and the plasticity index from 15.2% to 30.9%. The particle size and Atterberg's limits of soil M1 and S fell within the range recommended for earth construction (Table 3 and [56,57]). For soils K and M2, the clay contents and liquid limits of were above the recommended range, as highlighted in red in Table 3. However, the liquid limit showed a positive linear correlation with the clay fraction (< 2 μm) (R^2 =0.92), as previously observed [60]. Thus, supplementing soils K and M2 with sand could be an easy solution to reduce the clay fraction and the liquid limit in order to align with the recommended ranges.

The specific surface area obtained by the BET theory under a nitrogen atmosphere was comprised between 13 and 41 m^2/g for the four soils. Interestingly, the specific surface area positively linearly correlated with the passing at 63 μm (R^2 =0.97), as observed in Fig. 5. This outcome is likely attributed to the presence of aggregated clays within the silt fraction (2–63 μm) of tropical soils [58,59]. These aggregates, composed of kaolinite with iron and aluminium oxides, have been shown to affect the specific surface [61–63]. This strong correlation suggests that a fast and cost-effective evaluation of the passing at 63 μm could accurately indicate the specific surface area of weathered tropical soil.

The methylene blue test quantifies the absorption of methylene blue by 100 g of soil and is commonly used to assess the cation exchange capacity of clay. Methylene blue generally absorbs on the negatively charged basal surface of phyllosilicates [64] and, thus,

Table 3
Soil geotechnical characteristics.

	K	M1	M2	S	Recommended threshold[56,57]
Clay: < 2 μm (%)	49.7 ± 2.9	31.4 ± 0.5	42.1 ± 1.5	19.6 ± 1.7	8–32
Silt: 2–63 μm (%)	41.7 ± 6.3	9.2 ± 1.2	12.8 ± 1.3	40.5 ± 3.0	10–56
Clay + Silt: < 63 μm (%)	91.5 ± 0.2	40.7 ± 1.7	54.9 ± 0.8	60.1 ± 1.8	20–64
Sand: 63–2000 μm (%)	8.5 ± 0.2	59.3 ± 1.7	45.1 ± 0.8	39.9 ± 1.8	26–80
Texture (USDA triangle)	Silty clay	Sandy clay loam	Sandy clay	Loam	
D50 (μm)	2.0 ± 2.9	132.8 ± 1.5	9.1 ± 1.4	15.4 ± 0.3	
Liquid Limit LL (%)	72.9 ± 2.8	47.5 ± 0.6	62.6 ± 1.8	44.1 ± 1.9	25–50
Plastic Limit PL (%)	44.9 ± 4.9	22.3 ± 2.5	31.2 ± 2.8	28.9 ± 2.1	
Plasticity Index PI (%)	28.1 ± 4.5	25.2 ± 2.5	30.9 ± 3.7	15.2 ± 2.2	16–28
Methylene blue (g/100 g)	0.35 ± 0.00	0.29 ± 0.01	0.35 ± 0.03	0.15 ± 0.01	
Specific surface area (m^2/g)	40.78	13.23	16.55	23.04	

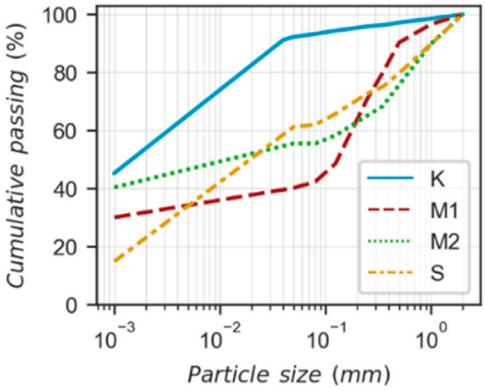

Fig. 4. Particle size distribution of the four soils.

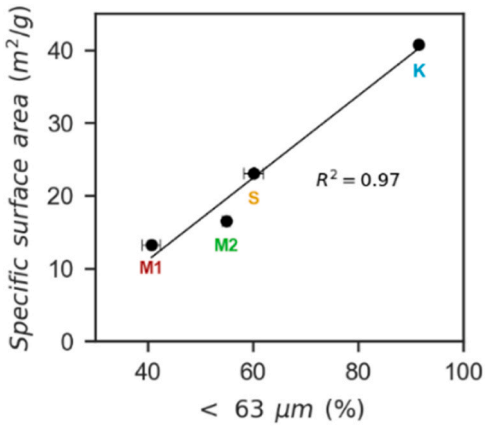

Fig. 5. Correlation between the passing at 63 μm and the specific surface area.

characterises the soil's ability to retain and exchange positively charged ions. Here, the methylene blue values of the four soils were very low, ranging from 0.15 to 0.35 g/100 g compared to values typically observed in temperate climates ranging from 0.5 to 1.7 g/100 g [65]. In weathered tropical soils, the negatively charged basal faces of phyllosilicates are covered by positively charged iron and aluminium oxides, which can result in a net positive charge. Therefore, methylene blue cannot absorb efficiently on tropical soils, which makes the test uninformative [6,66]. In temperate climate soils that are governed by negatively charged clays, the methylene blue test can generally provide reliable information on the specific surface area of the soil [67,68]. In contrast, in this study, no relationship was observed between the methylene blue value and the specific surface area (Table 3). This indicates that alternatives to the methylene blue test are needed for tropical soils.

3.2. Plastic earth mortar without dispersant

3.2.1. Influence of increasing water content on plastic earth mortar

The goal of this study was to determine the maximum compressive strength of earth mortars made without dispersant in order to assess the intrinsic resistance of each soil. For each soil, earth mortars were made with increasing water content between 20% and 70%. The physical characteristics of the fresh and hardened mortars are shown in Fig. 6. For each soil, the Optimal Water Content (OWC) corresponded to the water content resulting in the highest compressive strength.

Fresh mortar consistency prepared without dispersant fell within the plastic domain, and the yield stress was evaluated with the cone penetrometer test. Yield stress calculations were performed using the methodology detailed in [45] within the 70–0.75 kPa range, corresponding to a depth penetration between 3.5 and 34 mm. Due to their semi-solid consistency, measurements at low water content fell outside that range and were not reported (Fig. 6.a). For each soil, yield stress showed a linear log-log correlation with water content, consistent with prior research [45,69]. Soils S and M1 exhibited a similar decrease in yield stress with increasing water content, consistent with their closely matched plastic and liquid limits (Table 3). On the other hand, soils M2 and K required higher water content levels to decrease their yield stress, consistent with their higher plastic and liquid limit (Table 3).

Physical properties were evaluated on the dry mortars. Interestingly, important differences were observed between the soils. Soils K and S underwent important changes in compressive strength and dry density as the water content increased, around 2.5 MPa and

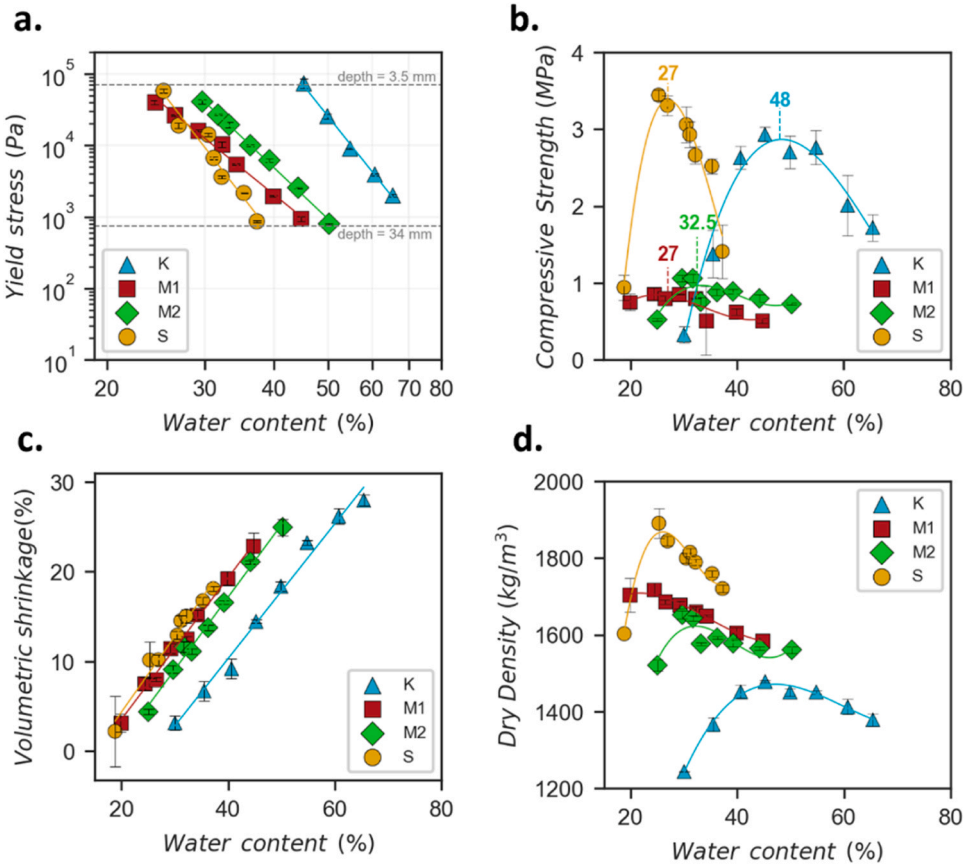

Fig. 6. Influence of water content on mortar properties.

250 kg/m^3 , respectively. In contrast, soils M1 and M2 showed only modest changes, around 0.5 MPa and 130 kg/m^3 , respectively. These differences may be attributed to the greater specific surface area of soil K and S, along with their distinctive mineral composition. In particular, soils K and S were rich in metal oxides that strongly interact with water [55], whereas soil M1 and M2 predominantly consisted of silicate minerals that have low interaction with water [55].

The volumetric shrinkage showed a positive linear correlation with water content (Fig. 6.c). This outcome aligns with traditional findings suggesting that the increase in initial water content leads to greater evaporation, augmenting porosity, and shrinkage [70–72]. The dry density and compressive strength exhibited the typical proctor compaction curve (Fig. 6.b/d). For each soil, dry density and compressive strength increased with water content until a maximum value before decreasing (Fig. 6.b). This expected result aligns

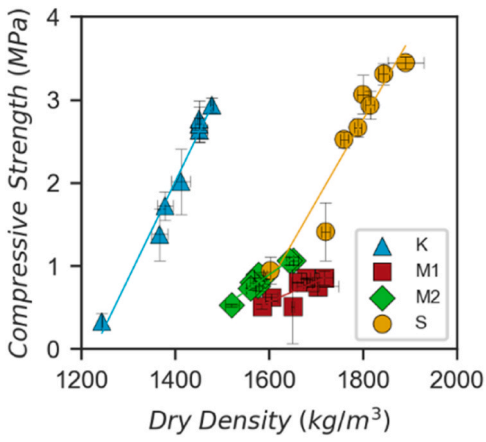

Fig. 7. Compressive strength versus dry density.

with observations made on earth material made with different shaping processes, such as compaction or casting [72–74]. In addition, as demonstrated by several studies [3,73,75], the compressive strength showed a positive linear correlation with the dry density (Fig. 7).

The OWC was selected based on the maximum compressive strength of the polynomial fitting curve, as shown in Fig. 6.b, M1 and S displayed the lowest OWC at 27%, followed by M2 at 32.5% and K at 48%. These OWC were used in the following sections to produce, characterise, and compare mortars at their highest strength.

3.2.2. *Earth mortar made at their OWC*

For each soil, the OWC closely matched the Atterberg plastic limit, differing by less than 5%. This observation is consistent with prior research that indicates that soils reach their highest solid volume fraction and, consequently, their maximum compressive strength near their plastic limit [17]. Interestingly, fresh earth mortars exhibited a similar consistency at their OWC, with an average yield stress of 22.5 ± 3.7 kPa (Fig. 8) corresponding to a depth penetration of 6.2 ± 0.5 mm.

This implies that a simple consistency test using a penetrometer test on fresh mortar (with < 2 mm soil) could offer good yield str in defining the OWC and the soil's highest packing density. Since measuring the plastic limit is often slow and imprecise, the penetrometer test on fresh mortar could represent a simpler and potentially more accurate alternative. As another benefit, the penetrometer test was conducted directly on the fresh mortar paste (<2 mm), while the plastic limit is measured on particles passing through a 400 μm sieve. This is consistent with other studies that advocate for evaluating water requirements directly on the whole soil paste instead of relying on plastic or liquid limits measured on modified particle size [10,11].

Inspired by a recent study predicting the yield stress of various soil pastes based on the solid volume fraction [12], a relationship was observed between the yield stress and the ratio of the water content to the OWC. The yield stress showed a linear log-log correlation with the ratio of water content to the OWC (R^2 >0.93) (Fig. 9).

This result implies that earth mortar yield stress could be predicted relying solely on water content and the OWC, which can be determined through a simple penetrometer test on fresh mortar. Given that adobe bricks share a similar consistency range to plastic earth mortar, these insights hold promise for controlling the consistency of adobe bricks.

The compressive strength of earth materials is attributed to capillary forces and ionic interactions between clay particles. Studies made on temperate climate soil showed that the clay fraction (<2 μm), the cation exchange capacity, the methylene blue value and specific surface area are positively linearly correlated with the compressive strength [10–12,18]. By contrast, these correlations were not observed in this study (Fig. 10.a/b/c). Instead, the compressive strength showed a strong positive linear with the total metal oxide content (R^2 =0.99) (Fig. 10.d) and the Fe_2O_3 content (R^2 =0.81) (Fig. 11.e). These results showed that the compressive strength increased with the metal oxide content, which aligns with previous research conducted on tropical soil [9,19,23,76–78]. This result is attributed to the ability of the iron and aluminium sesquioxides to aggregate and cement the other individual soil particles in the matrix, thereby improving soil cohesiveness [19,76,79]. Importantly, since the pH KCl and the total metal oxide content are highly correlated (Fig. 1), the compressive strength also correlated with the pH KCl (R^2 =0.99) (Fig. 10.f). This finding implies that a simple pH KCl measurement could predict the potential strength of earth mortar. This observation also highlights that the recent finding linking the compressive strength of earth materials with the methylene blue value and cation exchange capacity is only adapted for non-tropical soils with a net negative charge and likely cannot be used for positively charged tropical soils [10–12,18]. Consequently, the pH KCl could represent an alternative to the Methylene Blue rest for tropical soils.

The different soils reached their maximum compressive strength with an OWC ranging from 27% to 48%. OWC are known to correlate positively with the soil surface specific area, depending on the amount of water needed to cover the surface of all the grains and form a dense packing fraction [9–12]. Confirming these prior studies, the OWC correlated with the soil specific surface area of the four soils examined (R^2 =0.85) (Fig. 11.a). Furthermore, since the specific surface area and the passing at 63 μm are themselves correlated, (Fig. 5), the OWC showed a positive linear correlation with the passing at 63 μm (R^2 =0.84) (Fig. 11.b). This suggest that the passing at 63 μm could be used to estimate the optimal water content.

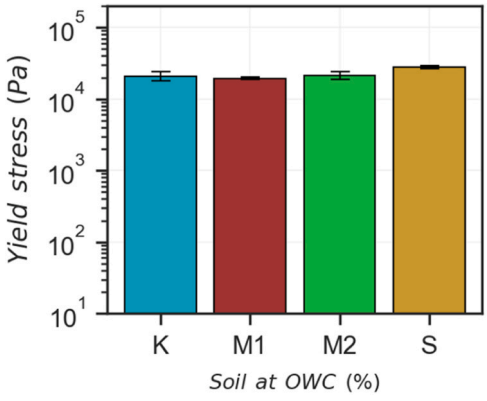

Fig. 8. Yield stress at OWC of the four soils.

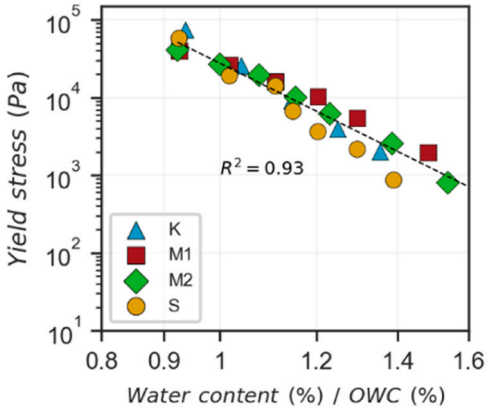

Fig. 9. Yield stress evolution of fresh mortar versus the water content divided by the OWC.

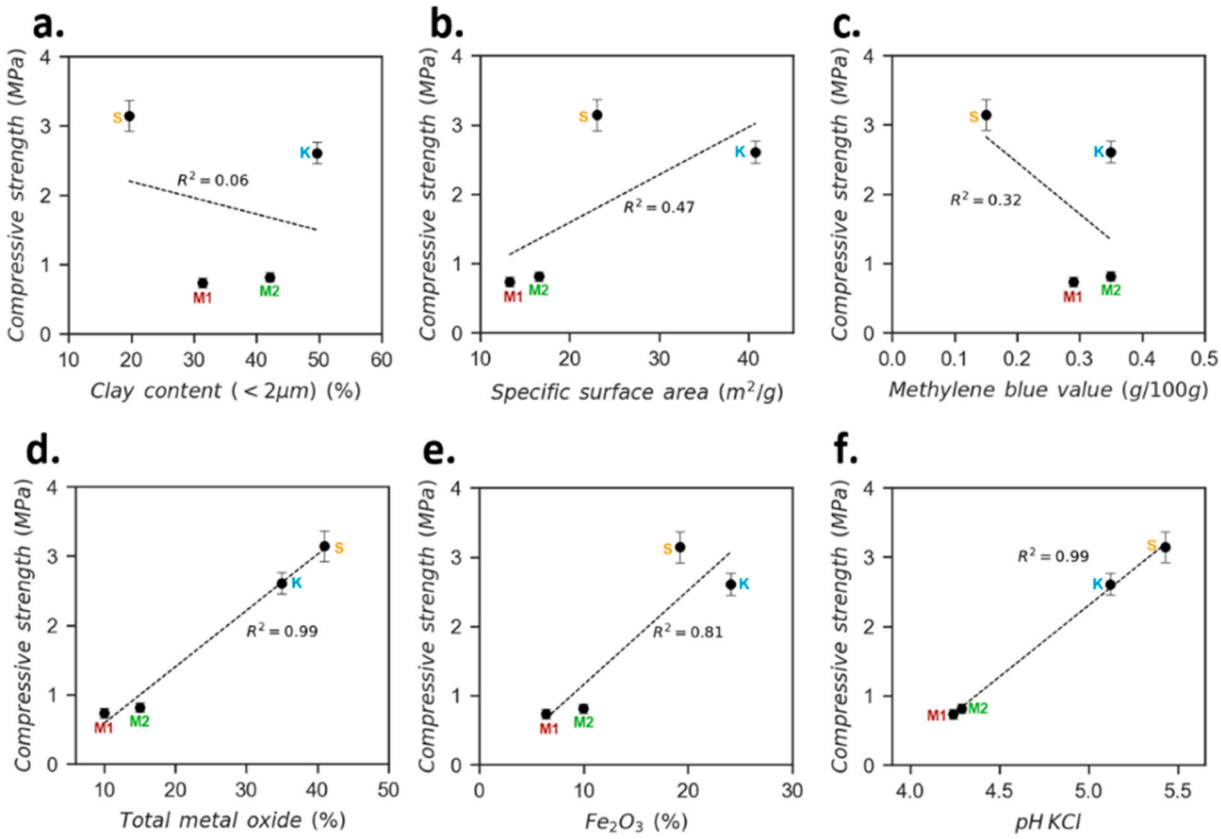

Fig. 10. Compressive strength versus clay content (a), specific surface area (b), Methylene blue value (c), Total metal oxide content (d), Fe_2O_3 (e), pH KCl (e) of the four plastic earth mortars made at their OWC.

Together, these results have significant implications for soil selection in tropical regions for earth construction materials manufacturing. It showed that the passing at 63 μm and the pH KCl could be used to quickly estimate the specific surface area and the metal oxide content of soils, and, in turn, predict the water requirement and the resulting mechanical properties.

3.3. Poured earth mortar with NaHMP

3.3.1. Establishing the optimum NaHMP content ($NaHMP_{opt}$)

The amount of dispersant required for complete soil deflocculation depends on the soil's particle size and mineralogy [13,32,36,

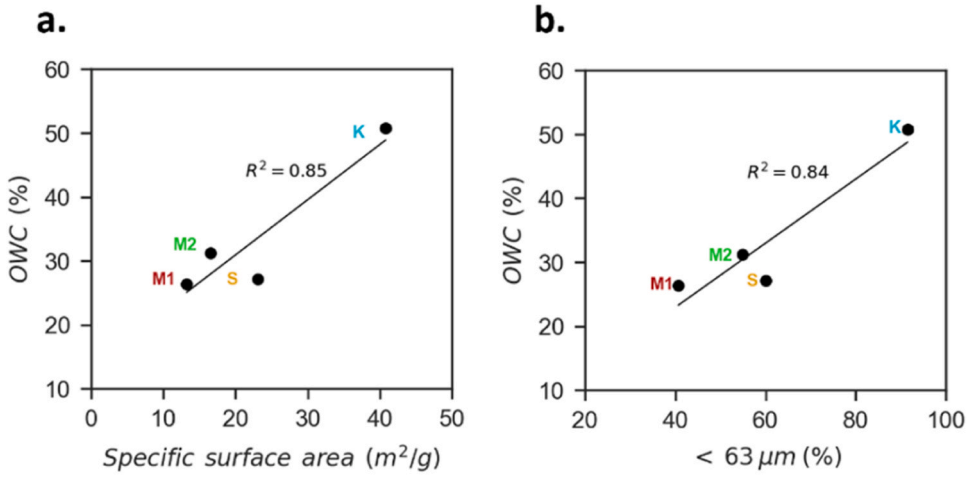

Fig. 11. OWC versus the specific surface area (a) and the passing at 63 µm (b).

37]. Increasing concentrations of NaHMP were tested on the consistency of the four earth (K, M1, M2, S) mortars made at their OWC. The yield stress was determined using a penetrometer test for plastic consistency (> 750 Pa) [45] and using a reduced-size Abrams cone for the fluid consistency (< 750 Pa) [47]. This approximate yield stress calculation provided a relevant order of magnitude and allowed for a good comparison between the experiments. Fig. 12 shows the decrease of the yield stress as a function of increasing NaHMP concentration for the four soils (K, M1, M2, S).

At 0% NaHMP, the yield stress of the four-earth mortar made at their OWC was around 20 kPa. As reported previously, the addition of NaHMP strongly decreased the yield stress of fresh mortars, until it reached a fluid consistency [17,28,30,31,38,73,80].

Previous studies have shown that a yield stress of 4 Pa corresponds to a maximum deflocculated state, and that further increases in NaHMP concentration had a limited effect on consistency but decreased compressive strength [38]. The $NaHMP_{opt}$ was defined as the lowest NaHMP concentration sufficient to reach a yield stress of 4 ± 0.5 Pa, corresponding in this study to a spread diameter of 41.5 ± 1 cm. The goal was to produce poured earth mortars at both their maximum deflocculated state and maximum compressive strength [38].

NaHMP's ability to deflocculate depends on the amount and type of clay particles [37]. Here, the $NaHMP_{opt}$ ranged from 0.25% to 1.4% for the four soils. Soil K and S had the highest $NaHMP_{opt}$ found at 1.4% and 0.9%, respectively, while M1 and M2 had a lower $NaHMP_{opt}$ at 0.25% and 0.26% respectively (Fig. 12). NaHMP induces deflocculation by increasing the overall negative surface being absorbed as an anion on the positive charge of phyllosilicate edge or positively charged metal oxide [37,38,80,81]. Soil K and S, the two positively charged and metal oxide-rich soil, required higher amounts of NaHMP than M1 and M2 to be deflocculated. This result aligns with other studies showing that higher amounts of dispersant are required to disperse positively charged iron and aluminium-rich soils [58,82]. Furthermore, soil K required a higher amount of NaHMP compared to soil S (Fig. 12). This result was attributed to a higher quantity of fine particles in soil K than in soil S, which, in turn, increased the specific surface area. Consequently, a higher NaHMP content was necessary in soil K to induce repulsion. Overall, these results suggested that NaHMP optimal concentration may be influenced by both the metal oxide content and the specific surface area. Confirming this hypothesis, $NaHMP_{opt}$ showed a strong positive linear correlation with the product of the specific surface area and the metal oxide content (R^2 =0.99) (Fig. 13.a). This result suggests that measuring the soil specific surface area and the metal oxide content could help predict the optimal NaHMP content. Furthermore, the analysis conducted above showed that the specific surface area correlated with the passing at 63 µm and that the metal oxide content correlated with the pH KCl. This suggest that the passing at 63 µm and the pH KCl could help predict $NaHMP_{opt}$. To confirm this hypothesis, $NaHMP_{opt}$ was further correlated with the passing at 63 µm and the pH KCl. As hypothesized, $NaHMP_{opt}$ showed a positive linear correlation with the product of the passing at 63 µm and the of pH KCl (R^2 =95) (Fig. 13.b). This important result suggests that the optimum concentration of NaHMP could be estimated with simple tests such as the passing at 63 µm and the pH KCl.

3.3.2. Poured Water Content (PWC) for poured mortar at their $NaHMP_{opt}$.

Following the determination of the $NaHMP_{opt}$ for each soil, the subsequent phase involved establishing the PWC required to produce a high-performance poured earth mortar. The PWC was defined as the water content required to achieve a suitable pouring consistency, fixed in this study at yield stress of 1000 Pa. The targeted yield stress was determined using the penetrometer test [45], corresponding to a depth penetration of around 29.5 cm and the Abrams slump test [47], corresponding to a slump of around 5.2 cm. The selection of the PWC required preliminary testing and was fixed when the yield stress from both determination methods (penetrometer depth and Abram's slump) fell within 1000 ± 300 Pa. The final mortar yield stress values made at their PWC are presented in Table 4. The yield stress values obtained from both methods closely align, validating the effectiveness of these simple techniques in reporting the yield stress of earth mortar, as supported by related studies [12,38,45,47,83].

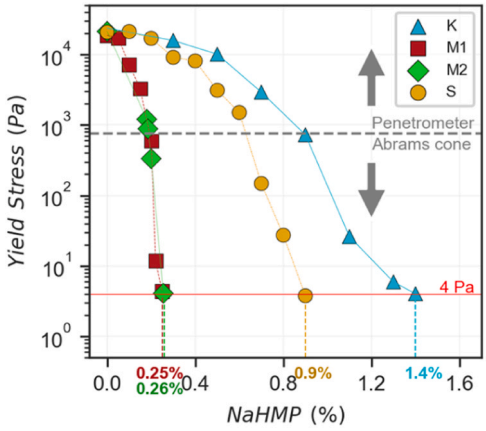

Fig. 12. Yield stress versus the NaHMP content.

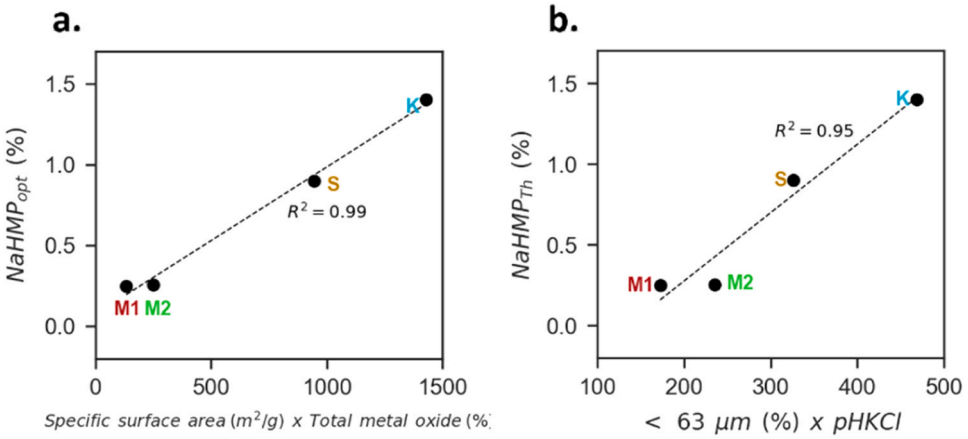

Fig. 13. $NaHMP_{opt}$ versus the product of specific surface area and total metal oxide content (a), versus of the product of the passing at 63 µm and the pH KCl (b).

Table 4
Yield stress determination via penetrometer and Abram's test for poured earth mortar.

Soil	K	M1	M2	S
Yield stress (Pa) penetrometer test	1122 ± 104	788 ± 12	906 ± 39	796 ± 21
Yield stress (Pa) Abrams slump test	994 ± 95	1040 ± 108	969 ± 125	969 ± 88
PWC (%)	39	19	26	19

3.3.3. Poured earth mortar properties

In Fig. 14, two types of mortar are compared based on their maximum strength achievable with or without a dispersant. Poured earth mortar made at their $NaHMP_{opt}$ and PWC, and plastic earth mortar made without a dispersant at their OWC. In line with findings from previous research [32,38,73], the use of a NaHMP resulted in a reduction in water content (Fig. 14.a) and an increase in compressive strength (Fig. 14.b) and dry density (Fig. 14.d). The water content showed a similar decrease of approximately 25% ± 5% (Fig. 14.a), accompanied by a similar dry density increase of approximately 9.9% ± 1.8%. The compressive strength of the poured earth mortar increased by over 50% compared to the earth mortar. However, it also displayed significant variability, with soils M1 and S showing an increase of around 180%, three times that of soils K and M2 around 60%. In contrast, the volumetric shrinkage of the poured earth mortar with dispersant either remained stable or decreased compared to that of the plastic earth mortar (Fig. 14.c). Fig. 14.e displays the ratio of four poured earth mortar properties to those of regular earth mortar, allowing for a rapid assessment of the dispersant's impact. When a property is greater than one (indicated by a black dotted circle) it indicates an increase between poured earth mortar and plastic earth mortar, while less than one means a decrease. As previously observed, adding a dispersant reduces water content and shrinkage while increasing dry density and compressive strength. Notably, this chart highlights the

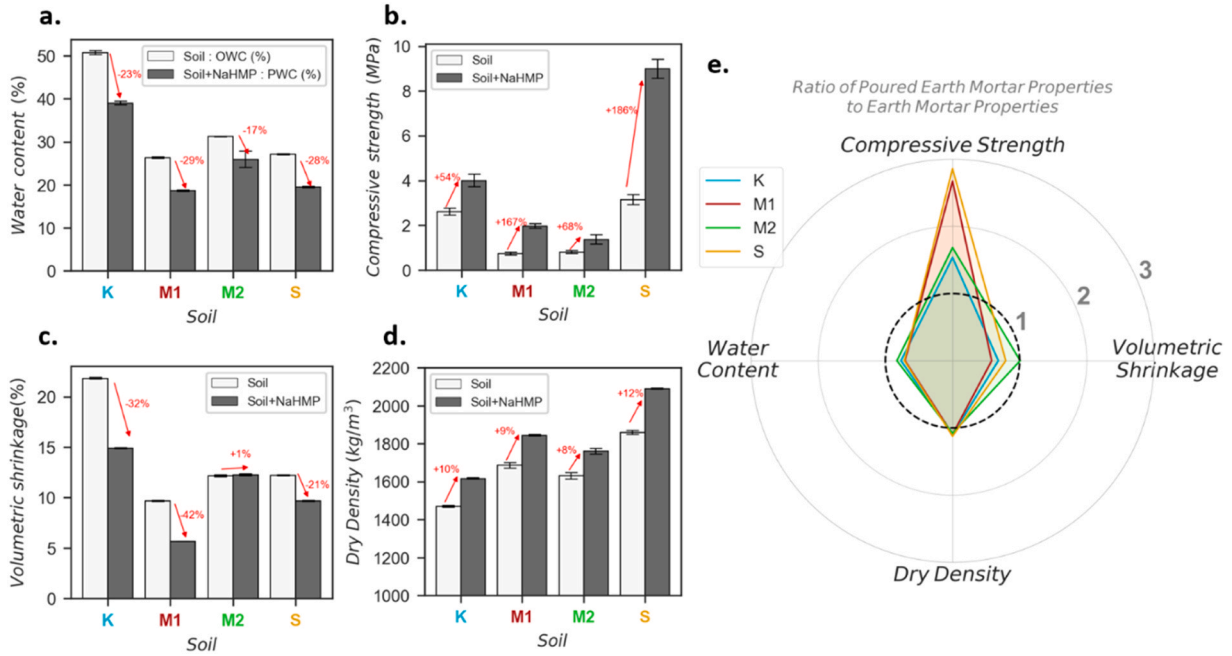

Fig. 14. Comparison of four mortar properties for earth mortar and poured earth mortar, water content (a), compressive strength (b), volumetric shrinkage (c), dry density (d), comparison of the four properties in a radar chart (e).

dispersant's most significant effect on compressive strength (Fig. 14.e). Most importantly, all measured properties of the poured earth mortar with dispersant were primarily related to their corresponding earth mortar properties without dispersant. Mortar properties from all four soil types, including water content, dry density, shrinkage, and compressive strength, maintained a consistent order of magnitude between the plastic earth mortar and the poured earth mortar. Regarding compressive strength, soil M1 and M2 had the lowest earth mortar compressive strength (< 1 MPa) and the lowest poured earth mortar compressive strength (<2 MPa). By contrast, soil K and S had the highest earth mortar without dispersant compressive strength (> 2 MPa) as well as the highest poured earth mortar compressive strength (> 4 MPa). This important finding suggests that the most critical criterion for formulating high-performance poured earth with NaHMP should be to initially select soils with high intrinsic resistance.

4. Conclusion

Achieving industrial-scale earth construction requires a shaping technique that competes with cement concrete and effectively manages soil variability within the design. Poured earth is a recent, easy-to-shape technique that requires a dispersant to improve the workability and hardened properties [24,30–33]. However, producing high-performance poured earth from variable soils is challenging. Particularly in tropical regions, there is a lack of comprehensive studies on the effects of soil on the properties of earth materials. This study investigated four tropical soils of French Guiana and their effect on the design and properties of poured earth mortar made with a dispersant (NaHMP). Results highlighted some key parameters allowing the prediction of earth mortar's fresh and hardened properties.

First, four tropical soils underwent comprehensive characterisation. Most notably, this analysis suggested that the passing at 63 μm and the pH KCl value could serve as effective proxies for the specific surface area and the metal oxide content. Subsequently, the study focused on plastic earth mortar without a dispersant and investigated the relationship between mortar and soil properties. Importantly, the compressive strength of the hardened earth mortar strongly correlated with the metal oxide content and could be estimated by the soil pH KCl. This result suggests that a simple measure of the soil pH KCl could be a discriminant test for selecting suitable tropical soils with high metal content and high compressive strength. Additionally, this study revealed that tests commonly used to characterize temperate climate soils, such as methylene blue tests, are not suitable for tropical soils with high metal oxide content, demonstrating the need for specific recommendations in tropical regions. Overall, the study highlights the potential of high strength poured earth construction made with tropical soils with high metal oxide content.

Using NaHMP to design poured earth mortars led to a reduction in water content and an increased in compressive strength and dry density. The optimal NaHMP concentration increased with the specific surface area and metal oxide content, and a strong correlation was observed between the optimal NaHMP concentration and the product of specific surface area and metal oxide content. This correlation was also robust when considering the product of pH KCl and the passing at 63 μm, both of which correlate with the specific surface area and the metal oxide content, respectively. Finally, this study examined poured earth mortars made at a reduced water content (PWC) to achieve a consistency similar to conventional vibrated cement concrete [40–42]. The strength, dry density, and water

content of poured earth mortar with dispersant correlated with those of plastic earth mortar without dispersant. Together, this underscores the importance of first examining plastic earth mortars made without dispersant, as their properties reliably predict those of poured earth mortar. For examples, soils with the highest compressive strength in plastic earth mortar also had the highest compressive strength when using NaHMP.

Additionally, the OWC, corresponding to the water content required to obtain the highest strength of plastic earth mortar, correlated with the specific surface area and the passing at 63 μm. Interestingly, the OWC was systematically found at a similar yield stress of 22 kPa (with a penetration depth of 6.2 mm). This result indicated that a simple penetrometer test could be used to adjust water content for optimal strength for designing plastic earth mortar, such as adobe brick. Furthermore, in poured earth mortars made with dispersant, the volumetric shrinkage showed a clear correlation with water content regardless of NaHMP use. This indicated that to minimize shrinkage of poured earth, it is essential to select soils with low water requirement.

Altogether, this study suggests that the simple measurement of the pH KCl and the clay and silt content (the passing at 63 μm) could be used to quickly screen and select tropical soils suitable for earth construction. As an example, among the four soils investigated here, the metal-oxide rich soils K and S, identified by pH KCl $>$ 4.8, exhibited the highest compressive strength in plastic earth mortar ($>$ 2.5 MPa) and poured earth mortar made with dispersant ($>$ 4 MPa). Between soils K and S, the lowest passing at 63 μm of soil S, 60% versus 90% for soil K, led to a lower water requirement, 19% versus 39%, and a lower volumetric shrinkage 15% versus 10%. This suggests that soil S is the most valuable soil identified in this study. To improve the validity of these results, tropical soil samples collected from other tropical regions of Africa and Asia will need to be studied.

CRediT authorship contribution statement

Walter Lily: Conceptualization, Data curation, Formal analysis, Investigation, Methodology, Supervision, Writing – original draft, Writing – review & editing. **Nait-Rabah Ouahcène:** Supervision, Validation. **Aubert Jean-Emmanuel:** Data curation, Supervision, Writing – review & editing. **Linguet Laurent:** Supervision, Validation. **Estevez Yannick:** Data curation, Supervision, Writing – review & editing. **Medjigbodo Gildas:** Supervision, Writing – review & editing.

Declaration of Competing Interest

The authors declare that they have no known competing financial interests or personal relationships that could have appeared to influence the work reported in this paper.

Data Availability

Data will be made available on request.

Acknowledgments

The authors wish to thank the French Guiana Ecological Transition Agency, the University of French Guiana, the Campus of Professions and Qualifications of Excellence of French Guiana, and the French Guiana Forest Ecology Research Unit for supporting this project.

References

[1] United Nations, Department of Economic and Social Affairs, Population Division, The World's Cities in 2018, in: 2018. ⟨https://www.un.org/en/development/desa/population/publications/pdf/urbanization/the_worlds_cities_in_2018_data_booklet.pdf⟩.
[2] Q.-B. Bui, J.-C. Morel, S. Hans, P. Walker, Effect of moisture content on the mechanical characteristics of rammed earth, Constr. Build. Mater. 54 (2014) 163–169, https://doi.org/10.1016/j.conbuildmat.2013.12.067.
[3] H. Houben, H. Guillard, Earth construction: a comprehensive guide, Practical Action Publishing, 1994.
[4] A.N. Ede, O.M. Olofinnade, E. Enyi-Abonta, G.O. Bamigboye, Implications of construction materials on energy efficiency of buildings in tropical regions, Int. J. Appl. Eng. Res. ISSN (2017).
[5] M.R. Hall, R. Lindsay, M. Krayenhoff, 1 - Overview of modern earth building, in: M.R. Hall, R. Lindsay, M. Krayenhoff (Eds.), Modern Earth Buildings, Woodhead Publishing, 2012, pp. 3–16, https://doi.org/10.1533/9780857096166.1.3.
[6] Tardy, Petrologie des laterites et des sols tropicaux, Masson, 1993.
[7] R. Anger, Approche granulaire et colloidale du matériau terre pour la construction, INSA De. Lyon (2011).
[8] L. Burros, The Nature and Properties of Soils. 11th edition. By Nyle C. Brady and Ray R. Weil. 1996. Prentice Hall, Inc., Upper Saddle River, NJ 07458. 740 pp. $85, hardcover, Am. J. Alternative Agric. 12 (1997) 45–45. ⟨https://doi.org/10.1017/s0889189300007189⟩.
[9] L. Walter, G. Medjigbodo, L. Claudot, O. Nait-Rabah, L. Linguet, Influence of metal oxides and particle size on earthen mortar built with tropical soils, Acad. J. Civ. Eng. 40 (2022) 1–10, https://doi.org/10.26168/ajce.40.2.34.
[10] N. Meimaroglou, C. Mouzakis, Cation Exchange Capacity (CEC), texture, consistency and organic matter in soil assessment for earth construction: The case of earth mortars, Constr. Build. Mater. 221 (2019) 27–39, https://doi.org/10.1016/j.conbuildmat.2019.06.036.
[11] M. Lagouin, J.-E. Aubert, A. Laborel-Préneron, C. Magniont, Influence of chemical, mineralogical and geotechnical characteristics of soil on earthen plaster properties, Constr. Build. Mater. 304 (2021), 124339, https://doi.org/10.1016/j.conbuildmat.2021.124339.
[12] D. Ardant, C. Brumaud, A. Perrot, G. Habert, Robust clay binder for earth-based concrete, Cem. Concr. Res. 172 (2023), 107207, https://doi.org/10.1016/j.cemconres.2023.107207.
[13] A. Julloux, C. Brumaud, G. Habert, A. Perrot, Variability of clay in poured earth, in: Dachverband Lehm eV (Ed.), LEHM 2020. Tagungsbeiträge Der 8. Internationalen Fachtagung Für Lehmbau, 2020. ⟨https://www.dachverband-lehm.de/lehm2020_online/pdf/lehm2020_p_brumaud-habert-julloux-perrot_en.pdf⟩.

[14] E. Anglade, J.-E. Aubert, A. Sellier, A. Papon, Physical and mechanical properties of clay–sand mixes to assess the performance of earth construction materials, J. Build. Eng. 51 (2022), 104229, https://doi.org/10.1016/j.jobe.2022.104229.
[15] A. Namdar, X. Feng, Evaluation of safe bearing capacity of soil foundation by using numerical analysis method, Fra&IntStrut. 8 (2014) 138–144, https://doi.org/10.3221/IGF-ESIS.30.18.
[16] A. Namdar, Natural minerals mixture for enhancing concrete compressive strength, Fra&IntStrut. 6 (2012) 26–30, https://doi.org/10.3221/IGF-ESIS.22.04.
[17] A. Perrot, D. Rangeard, A. Levigneur, Linking rheological and geotechnical properties of kaolinite materials for earthen construction, Mater. Struct. 49 (2016) 4647–4655, https://doi.org/10.1617/s11527-016-0813-9.
[18] H. Van Damme, M. Zabat, J.-P. Laurent, P. Dudoignon, A. Pantet, D. Gélard, H. Houben, Nature and distribution of cohesion forces in earthen building materials, Conserv. Anc. Sites Silk Road., Getty Publ. (2010) 181–188.
[19] S. Goldberg, Interaction of aluminum and iron oxides and clay minerals and their effect on soil physical properties: a review, Commun. Soil Sci. Plant Anal. 20 (1989) 1181–1207, https://doi.org/10.1080/00103629009368144.
[20] X.W. Zhang, L.W. Kong, X.L. Cui, S. Yin, Occurrence characteristics of free iron oxides in soil microstructure: evidence from XRD, SEM and EDS, Bull. Eng. Geol. Environ. 75 (2016) 1493–1503, https://doi.org/10.1007/s10064-015-0781-2.
[21] F. Bergaya, G. Lagaly, M. Vayer, Chapter 12.10 cation and anion exchange, in: F. Bergaya, B.K.G. Theng, G. Lagaly (Eds.), Developments in Clay Science, Elsevier, 2006, pp. 979–1001, https://doi.org/10.1016/S1572-4352(05)01036-6.
[22] M.E. Sumner, Measurement of soil pH: problems and solutions, Commun. Soil Sci. Plant Anal. 25 (1994) 859–879, https://doi.org/10.1080/00103629409369085.
[23] J. Camapum de Carvalho, L.R. de Rezende, F.B. da, F. Cardoso, L.C. de, F.L. Lucena, R.C. Guimarães, Y.G. Valencia, Tropical soils for highway construction: peculiarities and considerations, Transp. Geotech. 5 (2015) 3–19, https://doi.org/10.1016/j.trgeo.2015.10.004.
[24] L. Ronsoux, M. Moevus, Y. Jorand, S. Maximilien, C. Olagnon, R. Anger, L. Fontaine, Poured earth as concrete, HAL Arch. Ouvert. (2014).
[25] Y. Jorand, M. Mariette, L. Couvreur, D. Patrice, Environmental-Clay-based Concrete, in: Terra 2016, 2016.
[26] C.M. Ouellet-Plamondon, G. Habert, Self-Compacted Clay based Concrete (SCCC): proof-of-concept, J. Clean. Prod. 117 (2016) 160–168, https://doi.org/10.1016/j.jclepro.2015.12.048.
[27] Y. Du, G. Habert, C. Brumaud, Design of tannin based poured earth material via deflocculation-coagulation control: additives selection and tannin variation, (n. d.).
[28] A. Pinel, E. Prud'homme, A. Charlot, E. Fleury, Y. Jorand, Earthen construction: demonstration of feasibility at 1/2 scale of poured clay concrete construction, Constr. Build. Mater. 312 (2021), 125275, https://doi.org/10.1016/j.conbuildmat.2021.125275.
[29] H. Van Damme, H. Houben, Earth concrete, Stab. Revisit., Cem. Concr. Res. 114 (2018) 90–102, https://doi.org/10.1016/j.cemconres.2017.02.035.
[30] M. Moevus, Y. Jorand, C. Olagnon, S. Maximilien, R. Anger, L. Fontaine, L. Arnaud, Earthen construction: an increase of the mechanical strength by optimizing the dispersion of the binder phase, Mater. Struct. 49 (2016) 1555–1568, https://doi.org/10.1617/s11527-015-0595-5.
[31] A. Pinel, Y. Jorand, C. Olagnon, A. Charlot, E. Fleury, Towards poured earth construction mimicking cement solidification: demonstration of feasibility via a biosourced polymer, Mater. Struct. 50 (2017) 224, https://doi.org/10.1617/s11527-017-1092-9.
[32] M. Lagouin, A. Laborel-Preneron, C. Magniont, S. Geoffroy, J.-E. Aubert, Effects of organic admixtures on the fresh and mechanical properties of earth-based plasters, J. Build. Eng. 41 (2021), 102379, https://doi.org/10.1016/j.jobe.2021.102379.
[33] S. Guiheneuf, D. Rangeard, A. Perrot, Addition of bio based reinforcement to improve workability, mechanical properties and water resistance of earth-based materials, Acad. J. Civ. Eng. (Ed.), J. Augc. Asso. Fr. (2019) 184–192, https://doi.org/10.26168/icbbm2019.26.
[34] M. Kohandelnia, M. Hosseinpoor, A. Yahia, R. Belarbi, A new approach for proportioning self-consolidating earth paste (SCEP) using the Taguchi method, Constr. Build. Mater. 347 (2022), 128579, https://doi.org/10.1016/j.conbuildmat.2022.128579.
[35] G. Landrou, C. Brumaud, G. Habert, Influence of Magnesium on deflocculated kaolinite suspension: mechanism and kinetic control, Colloids Surf. A Physicochem. Eng. Asp. (2017).
[36] S. Guiheneuf, Formulation et renforts de blocs de terre crue pour une utilisation structurelle, l'institut national des sciences appliquées rennes, 2021.
[37] E. Castellini, C. Berthold, D. Malferrari, F. Bernini, Sodium hexametaphosphate interaction with 2:1 clay minerals illite and montmorillonite, Appl. Clay Sci. 83–84 (2013) 162–170, https://doi.org/10.1016/j.clay.2013.08.031.
[38] D. Ardant, C. Brumaud, G. Habert, Influence of additives on poured earth strength development, Mater. Struct. 53 (2020) 127, https://doi.org/10.1617/s11527-020-01564-y.
[39] P. Coudert, J. Barruol, B. Choubert, Carte geologique de la guyane. (1:100,000), (1958).
[40] J.A. Koch, D.I. Castaneda, R.H. Ewoldt, D.A. Lange, Vibration of fresh concrete understood through the paradigm of granular physics, Cem. Concr. Res. 115 (2019) 31–42, https://doi.org/10.1016/j.cemconres.2018.09.005.
[41] Z. Li, G. Cao, Rheological behaviors and model of fresh concrete in vibrated state, Cem. Concr. Res. 120 (2019) 217–226, https://doi.org/10.1016/j.cemconres.2019.03.020.
[42] D. Feys, G. De Schutter, R. Verhoeven, K.H. Khayat, Similarities and differences of pumping conventional and self-compacting concrete, in: Design, Production and Placement of Self-Consolidating Concrete, Springer, Netherlands, 2010, pp. 153–162, https://doi.org/10.1007/978-90-481-9664-7_13.
[43] C. Kabała, E. Musztyfaga, B. Gałka, D. Łabuńska, P. Mańczyńska, Conversion of soil pH 1:2.5 KCl and 1:2.5 HO to 1:5 HO: conclusions for soil management, environmental monitoring, and international soil databases, Pol. J. Environ. Stud. (2016).
[44] T.G. Fitton, K.D. Seddon, Relating Atterberg limits to rheology, in: Paste 2012: 15th International Seminar on Paste and Thickened Tailings, 2012 16–19 April, Sun City, Australian Centre for Geomechanics, 2012: pp. 273–284. ⟨https://doi.org/10.36487/ACG_rep/1263_23_Fitton⟩.
[45] A. Perrot, D. Rangeard, T. Lecompte, Field-oriented tests to evaluate the workability of cob and adobe, Mater. Struct. 51 (2018) 54, https://doi.org/10.1617/s11527-018-1181-4.
[46] T. Koumoto, G.T. Houlsby, Theory and practice of the fall cone test, Geotechnique 51 (2001).
[47] C.P. Roussel N, "Fifty-cent rheometer" for yield stress measurements: from slump to spreading flow, Soc. Rheol. (2005).
[48] Schwartzentruber, Catherine, La méthode du mortier de béton éuivalent (MBE) - Un nouvel outil d'aide a la formulation des bétons adjuvantés, Materials and Structures/Mat&iaux et Constructions. (2000).
[49] M. Duriez, F. Vieux-Champagne, R. Trad, P. Maillard, J.-E. Aubert, A methodology for the mix design of earth bedding mortar, Mater. Struct. 53 (2020) 16, https://doi.org/10.1617/s11527-020-1443-9.
[50] J.-Y. Li, R.-K. Xu, H. Zhang, Iron oxides serve as natural anti-acidification agents in highly weathered soils, J. Soils Sediment. 12 (2012) 876–887, https://doi.org/10.1007/s11368-012-0514-0.
[51] A.K. Dolui, P.P. Chattopadhyay, Extraction of forms of iron from some soil series of West Bengal and Bihar, Agropedology (1997).
[52] L. Tao, W. Zhang, H. Li, F. Li, Effect of pH and weathering indices on the reductive transformation of 2-nitrophenol in South China, Soil Sci. Soc. Am. J. (2012).
[53] J.-Y. Li, R.-K. Xu, K.-Y. Deng, Coatings of Fe/Al hydroxides inhibited acidification of kaolinite and an alfisol subsoil through electrical double-layer interaction and physical blocking, Soil Sci. 179 (2014) 495, https://doi.org/10.1097/SS.0000000000000093.
[54] J.Y. Li, R.K. Xu, Inhibition of acidification of kaolinite and an Alfisol by aluminum oxides through electrical double-layer interaction and coating, Eur. J. Soil Sci. 64 (2013) 110–120, https://doi.org/10.1111/ejss.12021.
[55] L.O. Filippov, L.A. Silva, A.M. Pereira, L.C. Bastos, J.C.G. Correia, K. Silva, A. Piçarra, Y. Foucaud, Molecular models of hematite, goethite, kaolinite, and quartz: Surface terminations, ionic interactions, nano topography, and water coordination, Colloids Surf. A Physicochem. Eng. Asp. 650 (2022), 129585, https://doi.org/10.1016/j.colsurfa.2022.129585.
[56] M.C. Jiménez Delgado, I.C. Guerrero, The selection of soils for unstabilised earth building: a normative review, Constr. Build. Mater. 21 (2007) 237–251, https://doi.org/10.1016/j.conbuildmat.2005.08.006.
[57] AFNOR, XP 13–901 Blocs de terre comprimée pour murs et cloisons: définitions - Spécifications - Méthodes d'essais - Conditions de réception, 2022.

[58] L.E.A.S. Suzuki, J.M. Reichert, J.A. Albuquerque, D.J. Reinert, D.R. Kaiser, Dispersion and flocculation of vertisols, alfisols and oxisols in Southern Brazil, Geoderma Reg. 5 (2015) 64–70, https://doi.org/10.1016/j.geodrs.2015.03.005.
[59] S.M. Barbosa, C.E. Carducci, M.E. Serafim, W.M. Zeviani, B. Albach, E. de, M. Castro, G.C. de Oliveira, Using ultrasonic and microwave devices to dry and disperse soils with high Fe2O3 content from Brazil, Geoderma Reg. 26 (2021), e00419, https://doi.org/10.1016/j.geodrs.2021.e00419.
[60] E. Polidori, Relationship between the atterberg limits and clay content, Soils Found. 47 (2007) 887–896, https://doi.org/10.3208/sandf.47.887.
[61] J.C. Mendez, E. Van Eynde, T. Hiemstra, R.N.J. Comans, Surface reactivity of the natural metal (hydr)oxides in weathered tropical soils, Geoderma 406 (2022), 115517, https://doi.org/10.1016/j.geoderma.2021.115517.
[62] M. Arias, T. Barral, F. Diaz-Fierros, Effects of iron and aluminium oxides on the colloidal and surface properties of kaolin, Clay and Clays, Minerals 4 (1995) 406–416.
[63] A. Eisazadeh, K.A. Kassim, H. Nur, Morphology and BET surface area of phosphoric acid stabilized tropical soils, Eng. Geol. 154 (2013) 36–41, https://doi.org/10.1016/j.enggeo.2012.12.011.
[64] J.A. Greathouse, D.L. Geatches, D.Q. Pike, H.C. Greenwell, C.T. Johnston, J. Wilcox, R.T. Cygan, Methylene blue adsorption on the basal surfaces of kaolinite: structure and thermodynamics from quantum and classical molecular simulation, Clays Clay Min. 63 (2015) 185–198, https://doi.org/10.1346/CCMN.2015.0630303.
[65] F. Rojat, E. Hamard, A. Fabbri, B. Carnus, F. McGregor, Towards an easy decision tool to assess soil suitability for earth building, Constr. Build. Mater. 257 (2020), 119544, https://doi.org/10.1016/j.conbuildmat.2020.119544.
[66] F. Aprile, R. Lorandi, Evaluation of cation exchange capacity (CEC) in tropical soils using four different analytical methods, J. Agric. Sci. 4 (2012) 278, https://doi.org/10.5539/jas.v4n6p278.
[67] Y. Yukselen, A. Kaya, Suitability of the methylene blue test for surface area, cation exchange capacity and swell potential determination of clayey soils, Eng. Geol. 102 (2008) 38–45, https://doi.org/10.1016/j.enggeo.2008.07.002.
[68] G. Kahr, F.T. Madsen, Determination of the cation exchange capacity and the surface area of bentonite, illite and kaolinite by methylene blue adsorption, Appl. Clay Sci. 9 (1995) 327–336.
[69] T.-W. Feng, A linear log - log w model for the determination of consistency limits of soils, Can. Geotech. J. 38 (2001) 1335–1342, https://doi.org/10.1139/cgj-38-6-1335.
[70] C.H. Kouakou, J.C. Morel, Strength and elasto-plastic properties of non-industrial building materials manufactured with clay as a natural binder, Appl. Clay Sci. 44 (2009) 27–34, https://doi.org/10.1016/j.clay.2008.12.019.
[71] E. Birle, D. Heyer, N. Vogt, Influence of the initial water content and dry density on the soil–water retention curve and the shrinkage behavior of a compacted clay, Acta Geotech. 3 (2008) 191–200, https://doi.org/10.1007/s11440-008-0059-y.
[72] E. Romero, A microstructural insight into compacted clayey soils and their hydraulic properties, Eng. Geol. 165 (2013) 3–19, https://doi.org/10.1016/j.enggeo.2013.05.024.
[73] A. Perrot, D. Rangeard, F. Menasria, S. Guihéneuf, Strategies for optimizing the mechanical strengths of raw earth-based mortars, Constr. Build. Mater. 167 (2018) 496–504, https://doi.org/10.1016/j.conbuildmat.2018.02.055.
[74] S. Leroueil, D.W. Hight, Compacted soils: from physics to hydraulic and mechanical behaviour (in:), Adv. Unsatur. Soils (2013), https://doi.org/10.1201/b14393-6.
[75] P. Zak, T. Ashour, A. Korjenic, S. Korjenic, W. Wu, The influence of natural reinforcement fibers, gypsum and cement on compressive strength of earth bricks materials, Constr. Build. Mater. 106 (2016) 179–188, https://doi.org/10.1016/j.conbuildmat.2015.12.031.
[76] X. Zhang, X. Liu, L. Kong, C. Chen, Role of free iron oxides in the physicochemical and mechanical properties of natural clay, Eng. Geol. 303 (2022), 106665, https://doi.org/10.1016/j.enggeo.2022.106665.
[77] E.S. Onwo, C. Emeh, O. Igwe, Effect of geochemical composition of lateritic soils on their geotechnical properties, Indian Geotech. J. 52 (2022) 877–894, https://doi.org/10.1007/s40098-022-00628-w.
[78] R.M. Madu, An investigation into the geotechnical and engineering properties of some laterites of Eastern Nigeria, Eng. Geol. 11 (1977) 101–125, https://doi.org/10.1016/0013-7952(77)90022-9.
[79] Y. Wang, Z.-Z. Cao, Y. Niu, H.-B. Lyu, Macromechanics, microstructure and particle contact model of artificially cemented laterite, Mater. Express 11 (2021) 732–739, https://doi.org/10.1166/mex.2021.1942.
[80] G. Landrou, C. Brumaud, M.L. Plotze, F. Winnefeld, G. Habert, A fresh look at dense clay paste: deflocculation and thixotropy mechanisms, Colloids Surf. A Physicochem. Eng. Asp. 539 (2018) 252–260, https://doi.org/10.1016/j.colsurfa.2017.12.029.
[81] F. Andreola, E. Castellini, J.M.F. Ferreira, S. Olhero, M. Romagnoli, Effect of sodium hexametaphosphate and ageing on the rheological behaviour of kaolin dispersions, Appl. Clay Sci. 31 (2006) 56–64, https://doi.org/10.1016/j.clay.2005.08.004.
[82] D. Pinheiro-Dick, U. Schwertmann, Microaggregates from Oxisols and Inceptisols: dispersion through selective dissolutions and physicochemical treatments, Geoderma 74 (1996) 49–63, https://doi.org/10.1016/S0016-7061(96)00047-X.
[83] T. Vinceslas, T. Lecompte, E. Hamard, A. Hellouin de Ménibus, H. Lenormand, T. Colinart, Methods to evaluate earth slip cohesion to build with light earth, Constr. Build. Mater. 238 (2020), 117665, https://doi.org/10.1016/j.conbuildmat.2019.117665.